SWELLING, CREEP AND THERMAL FATIGUE ANALYSIS FOR CYLINDRICAL FUSION REACTOR VACUUM WALL

B. M. MA

Department of Nuclear Engineering,
Iowa State University of Science and Technology, Ames, Iowa 50010, U.S.A.

SUMMARY

The vacuum-chamber wall or vacuum wall of a controlled fusion reactor will eventually be operated under severe conditions of irradiation damage, swelling, creep and thermal fatigue. The desirable wall material is an alloy of the refractory metals. For high thermal efficiency of the fusion reactor, the operating temperature range of the vacuum wall is expected to be from 600 to 1,000 °C.

Heat generation and temperature distribution in the wall are induced mainly from attenuation of neutrons and gamma rays. The most serious irradiation damage in the wall are dimensional and volumetric instabilities due to voids, bubbles and swelling of inert gases such as helium. The most important changes in mechanical properties of the wall material are: (a) ductility reduction, (b) enhanced irradiation creep, and (c) thermal fatigue due to cycling effect (especially for a pulsed fusion reactor). The objectives of this paper are to analyze the irradiation swelling, the creep stresses and strains and the lifetime of the vacuum wall resulting from severe irradiation, high temperature, and thermal fatigue.

Surface blistering and irradiation swelling are produced by deuterium, tritium and helium gases, and temperature gradients in the wall. The creep rate of the wall is greatly enhanced by irradiation damage and swelling. From the consideration of intensive radiation, high heat generation rate, large temperature variation, and enhanced creep rate, and on the basis of some basic assumptions, the irradiation swelling, creep stresses and creep strain rates can be analyzed.

Since the vacuum wall is subject to repeated thermal shocks and thermal loadings due to thermonuclear reactions of a controlled fusion reactor, thermal fatigue of the wall will occur. From some important factors of thermal cycling, the thermal fatigue can be analyzed and the lifetime of the vacuum wall may be predicted.

1. Introduction

A vacuum or first wall of the vacuum chamber (which contains and closely faces a thermonuclear plasma) of a controlled fusion reactor (possibly for use in the near future) is expected to be operated under severe condition of irradiation swelling, irradiation creep, and thermal-cycling fatigue. The first wall may be described as being between a thermonuclear plasma and a coolant-moderator-blanket material of the fusion reactor. In other words, the first wall of a controlled fusion reactor vessel (or vacuum chamber) is closely facing the thermonuclear plasma at the inner surface and has direct contact with the coolant-moderator-blanket material at the outer surface. The irradiation swelling, creep and thermal-cycling fatigue analysis for the first wall of controlled thermonuclear or fusion reactor (CTR) will be corresponding to the radiation, thermal and nuclianical analysis for pressure vessel of fission power reactors[1,2,3].

In the open-end systems (such as magnetic mirror devices) a controlled fusion reactor vessel generally has linear, cylindrical geometry. In the closed-end systems (such as stellarator and tokamak devices) a controlled fusion reactor vessel must have toroidal, cylindrical geometry. For different design concepts, the first wall and the vacuum wall of a fusion reactor vessel may refer to two different walls and locate at two different positions. In this paper, however, the vacuum wall of a long, cylindrical controlled fusion reactor vessel (or vacuum chamber) only will be concerned. At the same time, the first wall of the cylindrical vessel under the severe condition of irradiation swelling, irradiation creep, and thermal-cycling fatigue will be considered as a major component of the controlled fusion power reactor. The reactor vessel technology will also be closely associated with the fusion power reactor design and nuclear safety program.

The main objectives of this paper are

(1). To study the severe radiation effects on the first wall of a controlled thermonuclear (or fusion) reactor (CTR) under normal power operation condition

(2). To analyze the irradiation swelling and irradiation creep of the first wall and the related material properties of the wall

(3). To predict the stress range, strain range and cyclic life (or service lifetime) of the first wall due to thermal-cycling fatigue of CTR.

2. Radiation Damage

Radiation damage (or radiation-induced damage) to the first wall of a controlled fusion reactor vessel can be attributed to the bombardment, transmutation and diffusion of high-energy particles such as neutrons, alpha particles etc. For example, the deuteron ($^{2}_{1}D$) - triton ($^{3}_{1}T$) nuclear reaction for a controlled fusion reactor with deuterium tritium fuel

$$^{2}_{1}D + ^{3}_{1}T \longrightarrow \underset{(14.1\ \text{Mev})}{^{1}_{0}n} + \underset{(3.5\ \text{MeV})}{^{4}_{2}He} + 17.6\ \text{MeV (energy release)}$$

where the fast neutron ($^{1}_{0}n$) carries the kinetic energy of 14.1 MeV (million electron volts) and the α particle ($^{4}_{2}He$, helium atom) carries the kinetic energy of 3.5 MeV approximately. The sum of the kinetic energy carried by the two production particles is equal to the total energy release from the nuclear transmutation reaction. It is expected that for a fast neutron flux of 14.1 MeV of 2-3(10^{14}) neutrons per cm^2-sec (i.e., for a fluence of 10^{22}-

10^{23} neutrons per cm^2 in two years), the first wall will suffer from heavy bombardment and radiation damage. Also, the α -particle of 3.5 MeV will leave the plasma and deposit its energy or radiation in the first wall. In addition, the fast neutrons, n, can induce the (n, α), (n, 2n) and (n, nα) nuclear reactions with the elements present in the first wall. As a consequence, the particle bombardment, nuclear transmutation and helium diffusion will produce radiation damage resulting in void formation, dislocation defects and gas agglomeration inside the crystal structure of the wall material.

3. Void, Dislocation Formation and Irradiation Swelling

The formation of voids and dislocations in austinitic stainless stainless steel during fast neutron irradiation was first reported by Cawthorne and Fulton[4-5]. In the past few years, considerable progress has been made to characterize the structural damage over a wide range of irradiation environments. From experimental data available, various nucleation and growth models have been proposed. Those models may predict the void concentration, the spatial and size of void distributions, the effects of fast neutron flux, transmutation products, irradiation temperature and alloy composition on void and dislocation formation, and the volumetric change due to irradiation swelling qualitatively.

Nucleation and dislocation models proposed to explain void formation mechanisms mainly are (a) nucleation on pre-existing sites of dislocation, (b) nucleation in displacement or overlapping cascades, (c) nucleation by random fluctuations in vacancy clusters, (d) nucleation in displacement cascades stabilized by transmutation-produced helium, and (e) nucleation in vacancy clusters stabilized by existing inert gases (chiefly helium). At present, none of these nucleation models as well as void formation mechanisms have been treated analytically. The role of helium in the nucleation and void formation has not been well established. In general, the precipitation of helium may form bubbles (or blisters at wall surface). Such bubbles will grow by acquiring additional helium and vacancies at the dislocations. A bubble can reach a critical size at which it is dragged from the dislocation by the driving force due to thermal gradients[6].

The void nucleation, formation and growth (as well as bubble formation and growth) of inert gases can result in the volume change (i.e. volume increase or density decrease). In other words, the irradiation swelling can cause the volume increase in the first wall material. In order to fit the experimental data obtained from stainless steels irradiated in the EBR-II, some empirical equations are developed using the least-squares technique. An empirical equation for the void density, ρ_v, varying with the fast neutron fluence, ϕt, (or nvt) at three different irradiation temperature T (absolute) of austenitic stainless steel is given by

$$\rho_v = (\phi t)^{1.60 - 25/\theta + 150/\theta^2} \exp(10.25 - 0.015T) \qquad (3.1)$$

where ϕ is the fast neutron flux (n/cm^2 - sec), (> 0.1 MeV), t is the irradiation time (sec), v is the neutron velocity (cm/sec) and $\theta = T - 623$, the effective temperature. In the same manner, the empirical equations for mean void diameter, d, in Å, and volume change $\Delta V/V$ varying with fast neutron fluence at different irradiation temperatures are respectively expressed as

$$d = (\phi t)^{0.15 - 25/\theta^2} \exp(7.45 - 1700/T) \qquad (3.2)$$

$$\Delta V/V = 10^{-10} (\phi t)^{2.0 - 25/\theta - 75/\theta^2} (T - 40)\exp\left(-0.015T - \frac{5100}{T} + 32.5\right) \quad (3.3)$$

where V is the volume and ΔV is the volume increment of the specimen. The results calculated from Eqs. (3.1 - 3.3) to fit the experimental data are shown in Figs. 1-3. For purposes of comparison, the calculated results obtained by Brager et al[7] are shown in the dotted curves.

For given particle fluence and irradiation temperature, the volume change $\Delta V/V$ due to irradiation swelling may vary with the atom displacement damage. By using the least-squares fit, the volume change $\Delta V/V$ varying with the displacements per atom (dpa), N, can now be expressed by the simple empirical equation

$$\Delta V/V = c\, N^{1.2} \quad (3.4)$$

in which c is a coefficient (or parameter). The calculated results obtained from Eq. (3.4) and the experimental data observed for Type 316 stainless steel foil specimens irradiated at 773 and 873 ^{o}K with proton energies 0.75 - 1.0 MeV and proton fluence $6(10^{17})$ - $13(10^{22})$ protons/cm^2 are shown in Fig. 4. The coefficient $c = 1.7(10^{-3})$ at T = 773 ^{o}K and $c = 6.4(10^{-3})$ at T = 873 ^{o}K. The typical atom displacement damage rate related to the irradiation swelling is given in Table 1.

It should be noted that (a) the fast neutrons produced by the D-T nuclear reaction have energy about 14 MeV (much higher than 1 MeV), (b) the expected operating temperature for the first wall of a controlled fusion reactor vessel is in the range of 600 - 1000 ^{o}C, and (c) the first wall material may be an alloy of the BCC refractory material (instead of austenitic stainless steel).

In general, there are four main causes of irradiation swelling induced by the bombardment of high-energy particles (especially fast neutrons) in metals or metallic alloys in the different temperature regions:

(1) Nuclear transmutations (to produce helium)	all temperatures (decrease with T)
(2) Irradiation growth	$< 0.2\ T_{mp}$
(3) Void formation and growth	$0.3 - 0.5\ T_{mp}$
(4) Bubble formation and swelling	$\geq 0.5\ T_{mp}$

where T_{mp} is the absolute melting point temperature (^{o}K). The irradiation swelling breakaway in the first wall may occur when the irradiation temperature is in the neighborhood of $0.5\ T_{mp}$.

4. Probable Environment, Geometry and Material of the First Wall

The probable environment of the first wall of a cylindrical controlled fusion reactor vessel will be subject to:

(1). Intense radiation condition due to fast neutrons, primary gamma (or X-) rays, and small fractions of slow neutrons, secondary γ rays, α rays and β rays (from tritium diffusion).

(2). Radiation damage to induce void, dislocation formation and growth, bubble formation, surface sputtering, eroding and blistering, and irradiation swelling (as discussed above). The inner surface of the first wall may be protected by a thin-layer ceramic liner.

(3). Nuclear loading (or energy deposition) in the range from

1 MW/m^2 to 10 MW/m^2 (or 0.1 KW/cm^2 - 10 KW/cm^2)

(4). Operating temperature between 600 and 1000 ^{o}C.

(5). Partial vacuum between 10^{-2} and 10^{-5} Torr in the region adjacent to the inner surface of the first wall.

The geometry of the first wall is a circular cylinder or a tubular shell facing a thermonuclear plasma inward (as defined above). Of the first wall the inside diameter is between 2 and 6m, and the wall thickness is between 2.0 and 4.0 cm, depending on the reactor size, wall material, heat removal process, etc. A typical mechanical design of the first-wall sector for a controlled fusion reactor is shown in Fig. 5. The outer surface of the first wall is connected to the coolant channel (containing a coolant-moderator-blanket material i.e. Li or Li_2 Be F_4 salt) of the reactor. It is desirable that the difference between external coolant pressure and internal partial vacuum will produce tension in the inner region of the first wall and thus relieve probable compressive creep buckling of the first wall.

The selection of the material for the first wall will be a compromise based on a number of the important nuclear, physical, thermal, and mechanical properties, safety consideration and economic factors below:

Neutron flux $\phi = 5(10^{14}) - 5(10^{15})$ neutrons/cm^2-sec

Ion ($_1^1$H, $_1^2$D, $_1^3$T, etc) flux $5(10^{14}) - 10^{16}$ ions/cm^2-sec

Capture and scattering cross sections

Transmutational radioisotope production (especially helium)

Radioisotope decay heating rate

Gamma transitions and decay heat

Irradiation swelling rate

Surface sputtering rate

Permeability to deuterium and tritium gases

Erosion and corrosion rates (or resistances)

Melting point (probable operating temperature 600 - 1000 ^{o}C)

Thermal conductivity and diffusivity

Thermal expansion coefficient

Mechanical strength and ductility

Fabricability and reliability

Availability and cost

From the considerations of the important properties, safety and economics, the refractory materials: niobium, molybdenum and vanadium (see Table 2) satisfy the requirements. These elements will probably be used as alloys such as Nb-1Zr, Nb-10Zr, V-10Ti, V-5Ti-10Cr, Mo-5Ti, TZM, etc.

5. Heat Generation, Temperature Distributions and Irradiation Creep

Heat generation and temperature distributions in the first wall of a cylindrical controlled fusion reactor vessel are induced mainly from attenuation of fast neutrons, slow neutrons, primary gamma (or X-) rays and secondary gamma rays. The radiation source is the nuclear fusion reactions produced in a thermonuclear plasma. Neutron flux distributions and gamma dose rate intensity are related to the nuclear and physical properties for a given geometrical arrangement of the first wall. The temperature distributions in the first wall

can be determined when the heat generation rate from the attenuation of the neutrons and gamma rays is known[8].

Irradiation swelling caused by inert gases (especially helium) in the first wall is apparently a complicated problem. An analysis for the proposed model of irradiation swelling in oxide fuel elements of liquid-metal fast breeder reactor (LMFBR) has been introduced[6]. Inert gas atoms from voids, gas bubbles resulting from grain growths, and gas bubbles anchoring or leaving the dislocations and grain boundaries were treated. The general description of the proposed, analytical model for irradiation swelling can also be applied to the irradiation swelling in the first wall of controlled fusion reactor vessel.

The creep produced in an intensive radiation environment is called the irradiation creep. Nuclear radiation to cause irradiation creep in the first wall has two opposite effects: (a) irradiation hardening or helium embrittlement tends to increase hardness, mechanical strength and retard creep rate, but (b) nuclear transmutation produced and tritium decay developed inert gases (mainly helium) diffusing into the first wall appear to reduce mechanical strength and increase creep rate of the first wall. As the inert gases diffuse, agglomerate and accumulate in the first wall, its irradiation creep rate will also increase. Experimental data show that the rate of irradiation creep is highly enhanced by irradiation swelling.

6. Irradiation Creep Stress Analysis

In the stress analysis for irradiation creep of the first wall the following basic assumptions are made:

(1). The wall material under neutron and gamma irradiation remains isotropic and homogeneous

(2). The density of the wall material during irradiation creep is approximately constant

(3). The wall material obeys the von Mises yield criterion which satisfied experimental data for most metals and their alloys (including the refractory alloys)

(4). The state of plane strain is satisfied and the axial strain rate is practically zero

(5). The ratios of the principal shearing strain rates to the principal shearing stresses are constant.

From these assumptions the basic equations of displacement-strain rates, compatibility, incompressibility, yield condition, plane strain, stress equilibrium, and ratios of principal shearing strain rates to principal shearing stresses are established in the order:

$$\dot{\epsilon}_r = \frac{\partial \dot{u}}{r_i \partial x}, \qquad \dot{\epsilon}_t = \frac{\dot{u}}{r_i x} \tag{6.1}$$

$$\frac{\partial(x\dot{\epsilon}_t)}{\partial x} - \dot{\epsilon}_r = 0 \qquad \frac{\partial(x\epsilon_t)}{\partial x} - \epsilon_r = 0 \tag{6.2}$$

$$\dot{\epsilon}_r + \dot{\epsilon}_t + \dot{\epsilon}_z = 0, \qquad \epsilon_r + \epsilon_t + \epsilon_z = 0 \tag{6.3}$$

$$\dot{\epsilon}_z = 0, \qquad \epsilon_z = 0 \tag{6.4}$$

$$\sigma = \sigma_y = 2^{-1/2}[(\sigma_r - \sigma_t)^2 + (\sigma_t - \sigma_z)^2 + (\sigma_z - \sigma_r)^2]^{1/2} \tag{6.5}$$

$$\frac{\partial(x\sigma_r)}{\partial x} - \sigma_t = 0, \qquad x\frac{\partial\sigma_r}{\partial x} + \sigma_r - \sigma_t = 0 \tag{6.6}$$

$$\frac{\dot{\epsilon}_r - \dot{\epsilon}_t}{\sigma_r - \sigma_t} = \frac{\dot{\epsilon}_t - \dot{\epsilon}_z}{\sigma_t - \sigma_z} = \frac{\dot{\epsilon}_z - \dot{\epsilon}_r}{\sigma_z - \sigma_r} = \frac{3\dot{\epsilon}}{2k} \tag{6.7}$$

where

$\dot{u}$ = radial displacement rate of the first wall

$\dot{\epsilon}$ = effective strain rate of the wall

$\dot{\epsilon}_r$, $\dot{\epsilon}_t$, $\dot{\epsilon}_z$ = radial, tangential and axial strain rates

ϵ_r, ϵ_t, ϵ_z = radial, trangential and axial creep strains

$\sigma = \sigma_y$ = effective stress or yield stress

σ_r, σ_t, σ_z = radial, tangential and axial stresses

$x = r/r_i$, r, r_i = variable and inner radii of the wall

$k = \sigma/\dot{\epsilon}$ = dimensional constant

In Eqs. (6.2)-(6.4) the initial radial, tangential and axial creep strains have been assumed to be zero.

From the von Mises yield criterion, Eq. (6.5), the effective strain produced in the cylindrical first wall is given by

$$\epsilon = 1/3(2^{1/2})\,[(\epsilon_r - \epsilon_t)^2 + (\epsilon_t - \epsilon_z)^2 + (\epsilon_z - \epsilon_r)^2]^{1/2} \tag{6.8}$$

Introducing Eqs. (6.3) and (6.4) into Eq. (6.8), the effective creep strain or effective strain rate becomes

$$\dot{\epsilon} = 2(3^{-1/2})\dot{\epsilon}_t = -2(3^{-1/2})\dot{\epsilon}_r \tag{6.9}$$

$$\epsilon = 2(3^{-1/2})\epsilon_t = -2(3^{-1/2})\epsilon_r \tag{6.10}$$

whence

$$\dot{\epsilon} = -3^{1/2}(\dot{\epsilon}_r - \dot{\epsilon}_t), \quad \epsilon = -3^{1/2}(\epsilon_r - \epsilon_t) \tag{6.11}$$

Based on the conditions required by Eqs. (6.4) and (6.7), the axial stress becomes

$$\sigma_z = 1/2(\sigma_t + \sigma_r) \tag{6.12}$$

Substitution of Eq. (6.12) into Eq. (6.5) gives

$$\sigma = 1/2(3^{1/2})(\sigma_t - \sigma_r) \tag{6.13}$$

For a relatively thick first wall, $\sigma_t > \sigma_r$, so that the effective stress σ is always positive.

A combination of Eqs. (6.3), (6.4) and (6.11) yields

$$x\frac{\partial\sigma_r}{\partial x} = \sigma_t - \sigma_r = -\frac{2(\dot{\epsilon}_r - \dot{\epsilon}_t)}{3\dot{\epsilon}}\sigma = 2(3^{1/2})\sigma \tag{6.14}$$

From the first of Eqs. (6.3), (6.4) and (6.11), one obtains

$$\dot{\epsilon}_r = -\dot{\epsilon}_t = -1/2(3^{1/2})\dot{\epsilon} \tag{6.15}$$

Combining the first of Eq. (6.2) and Eq. (6.15) gives

$$\partial\dot{\epsilon}/\dot{\epsilon} = -2dx/x$$

Upon integration, a general solution for the effective creep strain rate is

$$\dot{\epsilon} = C_1(t)/x^2 \tag{6.16}$$

Similarly, from the second of Eqs. (6.2) - (6.4) and (6.11), a general solution for the effective creep strain is

$$\varepsilon = C_2(t)/x^2 \tag{6.17}$$

where $C_1(t)$, $C_2(t)$ are integration constants and t is time. By using the initial boundary conditions, t = 0, x = 1, then $\dot{\varepsilon} = \dot{\varepsilon}_i$ and $\varepsilon = \varepsilon_i$, the particular solutions for the effective strain rate and the effective creep strain are obtained

$$\dot{\varepsilon} = \dot{\varepsilon}_i/x^2, \quad \varepsilon = \varepsilon_i/x^2 \tag{6.18}$$

Eliminating x from these two equations, a relationship between the effective strain rate and the effective creep strain is established

$$\dot{\varepsilon} = \dot{\varepsilon}_i \varepsilon/\varepsilon_i \tag{6.19}$$

At the outside surface of the first wall (t = 0), $x = x_0$, then $\varepsilon = \varepsilon_0$ and $\varepsilon = \varepsilon_0$, so that Eq. (6.19) becomes

$$\dot{\varepsilon}_0 = \dot{\varepsilon}_i \varepsilon_0/\varepsilon_i \tag{6.20}$$

where $x_0 = r_0/r_i$, r_0 and r_i are outer and inner radii of the first wall, and $\dot{\varepsilon}_0$ and ε_0 are strain rate and creep strain at the outside surface of the first wall respectively. For gives values of ε_i and ε_i the effective strain rate and creep strain at any point in the first wall can be found. The values of ε_0 and ε_0 at x_0 can also be found from Eqs. (6.18). From Eqs. (6.18) the partial derivatives of $\dot{\varepsilon}$ and ε with respect to x are

$$\partial\dot{\varepsilon}/\partial x = -2\dot{\varepsilon}_i/x^3, \quad \partial\varepsilon/\partial x = -2\varepsilon_i/x^3 \tag{6.21}$$

Based on creep test data, a more general expression for the creep law correlating the effective stress σ, the effective creep strain ε and effective strain rate $\dot{\varepsilon}$ can be given by[9,10].

$$\sigma = f(\dot{\varepsilon},\varepsilon) \quad \text{or} \quad \dot{\varepsilon} = F(\sigma,\varepsilon) \tag{6.22}$$

Since $\dot{\varepsilon} = f(x,t)$, and σ is proportional to σ_r (see Eq. 6.13), the relationship between σ_r and $\dot{\varepsilon}$ (or ε) can be established. By differentiating σ_r with respect to $\dot{\varepsilon}$ or ε, a general relationship is

$$\frac{\partial\sigma_r}{\partial\varepsilon} = \frac{\partial\sigma_r}{\partial x} \Big/ \frac{\partial\varepsilon}{\partial x} \tag{6.23}$$

or

$$\frac{\partial\sigma_r}{\partial\varepsilon} = \frac{\partial\sigma_r}{\partial x} \Big/ \frac{\partial\varepsilon}{\partial x} \tag{6.24}$$

Substituting from Eqs. (6.14) and (6.21), performing the integration with appropriate limits and using the relationships obtained in Eqs. (6.18), Eqs. (6.23) or (6.24) yields

$$(\sigma_r)_x = -3^{-1/2} \int_{\dot{\varepsilon}_i}^{\dot{\varepsilon}_x} \frac{\sigma}{\dot{\varepsilon}}\, d\dot{\varepsilon} = -3^{1/2} \int_{\varepsilon_i}^{\varepsilon_x} \frac{\sigma}{\varepsilon}\, d\varepsilon \tag{6.25}$$

At the outside surface of the first wall where $(\sigma_r)_{x_0} = p$, Eq. (6.25) becomes

$$p = 3^{-1/2} \int_{\dot{\varepsilon}_i}^{\dot{\varepsilon}_o} \frac{\sigma}{\dot{\varepsilon}}\, d\dot{\varepsilon} = 3^{-1/2} \int_{\varepsilon_i}^{\varepsilon_o} \frac{\sigma}{\varepsilon}\, d\varepsilon \tag{6.26}$$

where p is the external equivalent pressure of the coolant-moderator-blanket material flowing outside the first wall. This external equivalent pressure is usually a designed pressure for heat removal from the first wall through the cooland of CTR.

For a given creep strain rate $\dot{\varepsilon}_i$ (or ε_i) at x_i ($x = 1$), from Eqs. (6.25) and (6.12) the radial, tangential and axial creep stresses are obtained

$$\sigma_r = p + 3^{-1/2} \int_{\dot{\varepsilon}_i}^{\dot{\varepsilon}_x} \frac{\sigma}{\dot{\varepsilon}} \, d\dot{\varepsilon} \tag{6.27}$$

$$\sigma_t = p + 3^{-1/2} \left[\int_{\dot{\varepsilon}_i}^{\dot{\varepsilon}_x} \frac{\sigma}{\dot{\varepsilon}} \, d\tilde{\varepsilon} + 2\sigma \right] \tag{6.28}$$

$$\sigma_z = p + 3^{-1/2} \left[\int_{\dot{\varepsilon}_i}^{\dot{\varepsilon}_x} \frac{\sigma}{\dot{\varepsilon}} \, d\dot{\varepsilon} + \sigma \right] \tag{6.29}$$

Dividing Eqs. (6.27)-(6.29) by the external equivalent pressure p, the dimensionless creep stress components are

$$\frac{\sigma_r}{p} = 1 + \frac{3^{-1/2}}{p} \int_{\dot{\varepsilon}_i}^{\dot{\varepsilon}_x} \frac{\sigma}{\dot{\varepsilon}} \, d\dot{\varepsilon}$$

$$\frac{\sigma_t}{p} = 1 + \frac{3^{-1/2}}{p} \left[\int_{\dot{\varepsilon}_i}^{\dot{\varepsilon}_x} \frac{\sigma}{\dot{\varepsilon}} \, d\dot{\varepsilon} + 2\sigma \right] \qquad 1 \le x \le x_0 \tag{6.30}$$

$$\frac{\sigma_z}{p} = 1 + \frac{3^{-1/2}}{p} \left[\int_{\dot{\varepsilon}_i}^{\dot{\varepsilon}_x} \frac{\sigma}{\dot{\varepsilon}} \, d\dot{\varepsilon} + \sigma \right]$$

These three components of the principal creep stresses produced in the first wall under high temperature and irradiation creep condition are now applied to the exponential function creep law.

7. Exponential Function Creep Law

Although most of the experimental creep and rupture data are plotted in the power function creep law, the hyperbolic sine creep law or exponential function creep law has been derived with sound grounds from theoretical analysis and supported by fundamental creep tests at relatively high temperatures (600 - 1000 °C). The exponential function creep law, i.e. the exponential stress-creep rate relationship, can be expressed as[11].

$$\dot{\varepsilon} = g\exp[\sigma/\sigma_{cm}] \text{ or } \sigma = \sigma_{cm} \ln(\dot{\varepsilon}/g) \tag{6.31}$$

in which σ_{cm} is the creep material modulus (similar to the reduced modulus in the plastic region of solids), and g is the combined creep rate enhancement factor representing mainly the effect of irradiation swelling on irradiation creep under intense radiation condition of the first wall[3]. The values of σ_{cm} and g can be chosen from simple tension creep tests under neutron irradiation environment (such as stainless steel creep specimens tested in the EBR-II reactor). For the first wall the progress of irradiation creep may often pass very quickly from the primary to the secondary stage of the creep.

By introducing Eq. (6.31) into Eq. (6.26) and integrating, the external equivalent pressure (for a given internal pressure or vacuum at the inner surface of the first wall) corresponding to the yield condition is

$$p = 1/2(3^{-1/2})\sigma_{cm}[\ln \frac{\dot{\varepsilon}_o}{\dot{\varepsilon}_i} - 2\ln g]\ln \frac{\dot{\varepsilon}_o}{\dot{\varepsilon}_i} \tag{6.32}$$

where the yield condition may have accomplished by the irradiation swelling and irradiation creep at the inner surface of the first wall. Substitution of the second of Eq. (6.31) into Eq. (6.30), after integration, yields

$$\frac{\sigma_r}{p} = -(\ln \frac{\dot{\varepsilon}}{\dot{\varepsilon}_i} - 2\ln g)/(\ln \frac{\dot{\varepsilon}_o}{\dot{\varepsilon}_i} - 2\ln g)$$

$$\frac{\sigma_t}{p} = \left[4\ln \frac{\dot{\varepsilon}}{g} - \ln \frac{\dot{\varepsilon}}{\varepsilon_i}(\ln \frac{\dot{\varepsilon}}{\dot{\varepsilon}_i} - 2\ln g)\right] \Big/ \ln \frac{\dot{\varepsilon}_o}{\dot{\varepsilon}_i}(\ln \frac{\dot{\varepsilon}_o}{\dot{\varepsilon}_i} - 2\ln g) \tag{6.33}$$

$$\frac{\sigma_z}{p} = \left[2\ln \frac{\dot{\varepsilon}}{\dot{\varepsilon}_i} - \ln \frac{\dot{\varepsilon}}{\dot{\varepsilon}_i}(\ln \frac{\dot{\varepsilon}}{\dot{\varepsilon}_i} - 2\ln g)\right] \Big/ \ln \frac{\dot{\varepsilon}_o}{\dot{\varepsilon}_i}(\ln \frac{\dot{\varepsilon}_o}{\dot{\varepsilon}_i} - 2\ln g)$$

which represent the radial, tangential and axial principal stresses of irradiation creep produced in the first wall of a cylindrical controlled fusion reactor vessel.

At the outer surface of the first wall, $x - x_o$ $\dot{\varepsilon} = \dot{\varepsilon}_o$, Eqs. (6.33) reduce to

$$\frac{\sigma_r}{p} = -1, \quad \frac{\sigma_t}{p} = \frac{4\ln(\dot{\varepsilon}_o/\dot{\varepsilon}_i)}{\ln \frac{\dot{\varepsilon}_o}{\dot{\varepsilon}_i}(\ln \frac{\dot{\varepsilon}_o}{\dot{\varepsilon}_i} - 2\ln g)} - 1, \quad \frac{\sigma_z}{p} = \frac{2\ln(\dot{\varepsilon}_o/\dot{\varepsilon}_i)}{\ln \frac{\dot{\varepsilon}_o}{\dot{\varepsilon}_i}(\ln \frac{\dot{\varepsilon}_o}{\dot{\varepsilon}_i} - 2\ln g)} - 1 \tag{6.34}$$

in which $(\sigma_t/p)_{x=1}$ is usually considered the maximum tangential stress (in tension for internal negative pressure) at the inner surface of the first wall.

8. Computation of Creep Stresses and Strain Rates

To apply these equations derived above for effective creep strain and strain rate, and the components of principal creep stress, a numerical example for the first wall of a long, cylindrical controlled fusion reactor vessel is chosen. Although the nuclear, physical and mechanical properties of the refractory metallic alloys such as Nb-10Zr, Mo-5Ti, V-20Ti etc. best meet the requirements of the first wall, an idealized material (or innovated stainless steel) will be selected to satisfy creep material constant required in the computation simultaneously. The radial dimensions, internal and external design pressures, nuclear, physical, and mechanical properties and combined creep rate enhancement factor are given in Table 3.

The computed results obtained from a computer program are shown by graphs. Figure 6 shows that the effective creep strain and strain rate vary with the first wall thickness, while Figs. 7 and 8 give the radial, tangential and axial creep stresses varying with the first wall thickness. Figure 9 shows the maximum tangential creep stress (at x = 1) varying with the creep rate at $x_o = 1.10$ and 1.20 respectively.

9. Thermal-cycling Fatigue

Thermal cycling induced by nuclear reactor kinetics is an inherent character of all fission and fusion reactors, particularly the pulsed-type reactors. In CTR, the phenomenon of thermal cycling can be developed from repeated changes in temperature during repetitive fuel or energy replacement time. In fact, both theta pinch and tokamak devices are expected

to be operated as pulsed-type fusion reactors for power generation.

Material fatigue will take place when a specimen undergoes repeated mechanical and/or thermal loading. Thermal fatigue is usually caused by thermal loading due to cyclic temperature. Thermal-cycling fatigue (or low-cycle thermal fatigue) may be defined as the process whereby cracks originate and are propagated in materials which have cyclic temperature and thermal strain (or stress) at elevated temperature.

The creep stresses developed in the first wall (during normal operation of a pulsed or unsteady fusion reactor) combined with hydrogen-isotope absorption and helium diffusion can be related to the thermal fatigue. As the interrelations between void, dislocation and gas-bubble formation, irradiation swelling, and irradiation creep in the first wall, the hydrogen-isotope absorption and helium diffusion at the cracks in the first wall can cause fatigue failure through brittle fracture. Hydrogen-isotope absorption may be a function of the creep stresses. Helium production and diffusion from tritium decay may be comparable to the helium generation rate from (n, α) transmutation reactions when tritium concentration in the first wall is sufficiently high (about 4,000 ppm). Helium embrittlement can spread and accelerate thermal-cycling fatigue to fracture failure. On the other hand, interstitial and vacant point defects might be swept up and absorbed by oscillating dislocation due to thermal cycling. Large thermal fatigue strains might reduce voids, bubbles and irradiation swelling. The possible modification in swelling due to creep and fatigue and vice versa may be varified experimentally.

10. Thermal Fatigue Analysis

Among the basic equations for irradiation creep stress analysis, the compatibility and equilibrium equations (for example, Eqs. 6.2 and 6.6) can be utilized in the thermal-cycling fatigue or thermal fatigue analysis. These compatibility and equilibrium equations, independent of material constants, are applicable to both elastic and plastic (or creep and fatigue) regions of wall materials. To solve these equations interrelations between stresses and total fatigue strain are required.

Experimental data obtained from fatigue behavior of AISA 4130 steel and others under strain cycling show that the relation between elastic strain range per cycle, ϵ_e, and corresponding cyclic life (or number of cycles to failure), N_f, can be represented by the asymtotic stress-strain curve, (Fig. 10).

$$\epsilon_e = \frac{\sigma_e}{E} N_f^y \tag{10.1}$$

where E is the elastic modulus, σ_e and y are the elastic material constants. Equation (10.1) satisfies the cyclic life range up to 10^6 cycles for a large number of materials tested.

Similarly, test results observed from fatigue behavior of annealed AISA 4130 steel and other similar materials indicate that the relation between plastic strain range per cycle, ϵ_p, and corresponding cyclic life N_f can be expressed as [12], (Fig. 11).

$$\epsilon_p = mN_f^z \tag{10.2}$$

in which m and z are the plastic material constants. The exponent z was suggested as a parameter, differing from tested materials and varying from -1/3 to -1/2. The value z = -1/2 is better satisfied.

In many practical applications, the total strain range per cycle, ϵ, (or $\Delta\epsilon$), is of

interest. Therefore, the relation between total strain range and cyclic life can be obtained by adding Eqs. (10.1) and (10.2)

$$\epsilon = \Delta\epsilon = \epsilon_e + \epsilon_p = \frac{\sigma_e}{E} N_f^y + mN_f^y \tag{10.3}$$

where $\Delta\epsilon$ is the finite strain range between any two consecutive cycles under the asympotically linear condition as shown in Fig. 12.

The principal need in design analysis and calculation of thermal fatigue is a relation between stress range $\Delta\sigma$ and total strain range $\Delta\epsilon$. Such a relation can provide a means of combining the strain compatibility and stress equilibrium equations together. By eliminating N_f from Eqs. (10.1) and (10.2) and combining with Eq. (10.3), the result is

$$\Delta\epsilon = \frac{\Delta\sigma}{E} + m\left(\frac{\Delta\sigma}{\sigma_e}\right)^{z/y} \tag{10.4}$$

where $\Delta\sigma$ is usually taken as the asymptotic stress range at the half-life ($N_f/2$) of a specimen. From the logarithmic plots of elastic strain range and plastic strain range versus cyclic life (see Eqs. 10.1, 10.2, Figs. 10 and 11), the elastic and plastic material constants, σ_e, y, m and z of specimens can be determined experimentally. Hence, the strain range, stress range, and the cyclic life can be predicted from Eqs. (10.1)-(10.4).

It is well-known that there is a critical stress, usually called endurance limit, σ_u, in the elastic stress versus cyclic life curve (or the S-N curve) observed from fatigue tests. Below the critical stress or endurance limit, no plastic flow will take place and the cyclic life can be kept infinite. When the endurance limit is reached and plastic flow develops, however, the cyclic life becomes finite. Thus, the stress range (or stress amplitude) at the endurance limit is $2\sigma_u$. If a power function law exists between the plastic flow and the stress range, then the plastic strain range per cycle can be expressed as

$$\epsilon_p = M(\Delta\sigma - 2\sigma_u)^n \tag{10.5}$$

where M is the proportional material modulus and n is an integer of the power function. Introducing Eq. (10.2) into Eq. (10.5) and solving for $\Delta\sigma$ give

$$\Delta\sigma = 2\sigma_u + (\epsilon_p/M)^{-n} = 2\sigma_u + \left(\frac{m}{M}\right)^{-n} N_f^{z/n} \tag{10.6}$$

Dividing by the elastic modulus E, the relation of $\Delta\sigma$ in terms of strain becomes

$$\frac{\Delta\sigma}{E} = \frac{2\sigma_u}{E} + \frac{1}{E}\left(\frac{m}{M}\right)^{-n} N_f^{z/n} \tag{10.7}$$

For given values of σ_u, E, M and n, Eqs. (10.4) can be combined with Eqs. (10.6) and (10.7) to predict the desired results of strain range, stress range and cyclic life of the first wall material.

In a more general case, the material constants σ_e, σ_u, m, M, n, y and z which vary from material to material can best be determined experimentally from thermal-cycling fatigue tests of the wall material in an intensive radiation environment. Equations (10.1)-(10.7) can be used to the advantage for thermal-cycling fatigue analysis of the first wall.

11. Conclusions

From the preceding analysis for irradiation swelling, irradiation creep and thermal-cycling fatigue of the first wall of CTR vessel, the following conclusions are drawn:

(1). The first wall will suffer from heavy radiation damage of fast neutrons, primary

gamma (or X-) rays and charged particles produced by the controlled fusion reactions in a thermonuclear plasma.

(2). The void, dislocation and bubble formation, agglomeration and growth of inert gases (mainly helium) induced by radiation can result in severe irradiation surface blistering and volume swelling of the first wall (if a thin-layer ceramic liner for the surface protection is not used). The void density, mean void diameter and volume (or density) change in the first wall increase with the neutron fluence (or radiation intensity), irradiation temperature, and/or atomic displacement damage of the wall material (see Eqs. 3.1-3.4). The irradiation swelling breakaway in the first wall may occur when the irradiation temperature is in the neighborhood of half melting point temperature of wall material under operation condition.

(3). Irradiation swelling can highly enhance creep strain rate in the first wall. The creep strain and strain rate decrease with increasing first wall thickness (Fig. 6). The components of the principal creep stress and the maximum tangential creep stress (in tension) also decrease with increasing first wall thickness to a certain limit (Figs. 7-9). The maximum tensile tangential stress produced at the inner surface of the first wall will prevent any compressive creep buckling in the wall.

(4). Thermal cycling induced by nuclear reactor kinetics is an inherent character of controlled fusion (as well as fission) reactors, particularly the pulsed-type reactors. In the thermal-cycling fatigue analysis the elastic and plastic strain ranges, stress range, and cyclic life of the first wall can be predicted after the material property constants are determined experimentally (Equations 10.1-10.7).

(5). The synergistic effects of hydrogen-isotope absorption, helium production (from tritium decay and nuclear transmutation reactins), inert gas diffusion, bubble formation and irradiation swelling on the material properties of the first wall can greatly interact with the irradiation creep and the thermal-cycling fatigue of the wall. Since irradiation creep can relieve thermal stress as well as thermal-cycling fatigue, these synergistic effects may sufficiently modify the mechanisms of irradiation creep and thermal-cycling fatigue in the first wall. Radiation alleviation, temperature control, material compatibility, stress relaxation, strain limit, etc. need to be considered carefully for the first wall of a controlled fusion reactor vessel.

ACKNOWLEDGMENT

The author wishes to express his appreciation to Dr. Glenn Murphy, Department of Nuclear Engineering, Dr. David R. Boylan, Dr. Paul W. Peterson, and others, in the College of Engineering and Engineering Research Institute of ISU for their encouragement in the preparation of the paper.

References

1. Ma, B. M., "Thermal and Pressure Stresses in Cylindrical Reactor Pressure Vessels," Nuclear Engineering and Design 11, 416-426. (1970).

2. Ma, B. M., "Creep Stress Distribution in Long, Cylindrical Reactor Pressure Vessels," The Pressure Vessels and Piping Conference, American Society of Mechanical Engineers, San Francisco, May 10-12, Paper No. 71-PVP-29. (1971).

3. Ma, B. M., "Plastic Stresses and Strains in Cylindrical Reactor Pressure Vessels," Proc. First International Conference on Structural Mechanics in Reactor Technology, 4: Part G, G1/5, 65-91 (1971).

4. Cawthorne, C., and E. J. Fulton, "The Influence of Irradiation Temperature on the Defect Structures in Stainless Steel," Atomic Energy Research Establishment, Harwell, Report AERE-R-5269, (1967).

5. Cawthorne, C. and E. J. Fulton, "Voids in Irradiated Stainless Steel," Nature, 216, 575-576, (1967).

6. Cheng, C. K. and B. M. Ma, "Thermal Radiation and Mechanical Analysis for Unsteady-State Fuel Restructuring of Cylindrical Oxide Elements in Fast Reactors," Nuclear Science and Engineering, 48, 139-158 (1972).

7. Brager, H. K., J. L. Straalsund, J. J. Holmes, and J. F. Bates, "Irradiation-Produced Defects in Austenitic Stainless Steel," USAEC Report WHAN-FR-16, WADCO, (1970).

8. Ma, B. M., "Heat Generation and Temperature Distributions in Cylindrical Reactor Pressure Vessels," Nuclear Engineering and Design 11; 1-15 (1969).

9. Bailey, R. W., "Creep Relationships and Their Applications to Pipes and Cylindrical Parts under International Pressure," Proc., Institution of Mechanical Engineers, England, 164, 425-431 (1951).

10. Ma, B. M., "A Power-Function Creep Analysis for Rotating Solid Disks Having Variable Thickness and Temperature," Journal of the Franklin Institute, 277, 593-612 (1964).

11. Ma, B. M., "A Creep Analysis of Rotating Solid Disks," Journal of the Franklin Institute, 267, 149-165 (1959).

12. Manson, S. S., "Behavior of Materials under Conditions of Thermal Stress," NACA Technical Note TN 2933 (1954).

Table 1. Typical Atom Displacement Damage Rate Related to Irradiation Swelling

Radiation source	Maximum point defect production rate in Nb 10^{-6} dpa/sec
Controlled thermonuclear or fusion reactor (CTR) nuclear loading 10Mw/m^2	4.4
Fast Flux Test Facility (FFTF)	3.0
The Experimental Breeder Reactor II (EBR-II)	1.6
High Flux Isotope Reactor (HFIR)	1.3
Dynamitron, 4 MeV proton	10-100

Table 2. Comparison of Relavant Properties for Prospective First Wall Materials

Property	Niobium Nb	Molybdenum Mo	Vanadium V	Fe-Ni Base Alloys
Neutron capture cross section (> 1 MeV)	Low	Moderate	High	Mod.-high
Irradiation swelling rate	Low-Mod.	Low	Low	Moderate
Decay heat generation	High	Moderate	Low	Moderate
Thermal conductivity	High	High	High	Low-mod.
Thermal diffusivity	High	High	High	Moderate
Approximate melting point (°C)	2400	2600	1900	1500
Mechanical strength	Moderate	High	High	High
Ductility	Low	Moderate	Moderate	High
Corrosion resistance (to Li)	High	High	Medium	Med.-poor
Sputtering rate	Low	High	Low	High
Tritium and helium diffusion	High	Low	Very high	Low
Fabrication cost	High	Medium	High	Low
Availability	Limited	Common	Common	Very common

Table 3. Design Data for the First Wall of CFR Vessel

Notation	Description	Magnitude and Units
r_i	Inner radius	2 meters
r_o	Outer radius	2.2, or 2.4 meters
P_i	Internal design pressure	1.4 (10^{-5}) Kg cm^{-2} (10^{-3} Torr)
P	External equivalent pressure	75 Kg cm^{-2}
$\phi = \phi_n$	Fast neutron flux	5(10^{14}) - 5(10^{15})n cm^{-2} sec^{-1}
ϕ_γ	Gamma flux	5(10^{12}) - (10^{14}) γ cm^{-2} sec^{-1}
Σ	Neutron absorption coefficient	0.10 cm^{-1}
ν_e	Gamma energy absorption coefficient	0.140 cm^{-1}
ρ	Wall material density	7.88 gm cm^{-3}
T	Average operating temperature	800 °C (1073 °K)
k	Thermal conductivity	10.45(10^{-2}) cal cm^{-1} sec^{-1}C
K	Thermal diffusivity	9.52 (10^{-2}) cm^2 sec^{-1}
h	Boundary conductance	5.45 (10^{-1}) cal cm^{-2} sec^{-1} C
σ_y	Yield point strength (at 800 °C)	2.000 Kg cm^{-2}
σ_{cm}	Creep material modulus (or number)	500 Kg cm^{-2}
g	Combined creep rate enhancement factor	10^{-8} cm cm^{-1} day^{-1}
ε_i	Creep rate at the inner wall surface	0.10 cm cm^{-1}

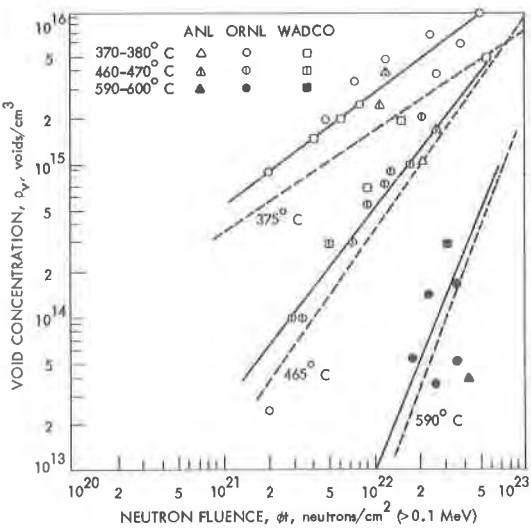

Fig. 1. Void concentration varies with neutron fluence for annealed 304 stainless steel.

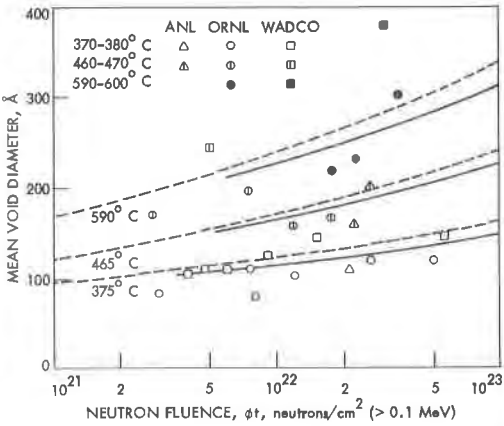

Fig. 2. Mean void diameter varies with fast-neutron fluence for annealed 304 stainless steel.

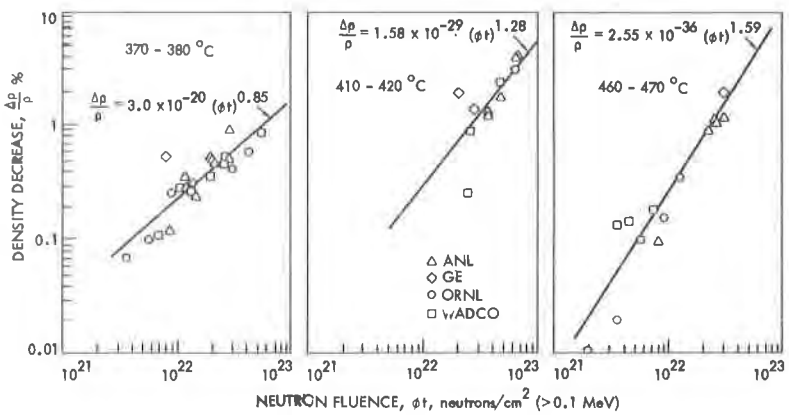

Fig. 3. Density decrease varies with neutron fluence for annealed 304 stainless steel.

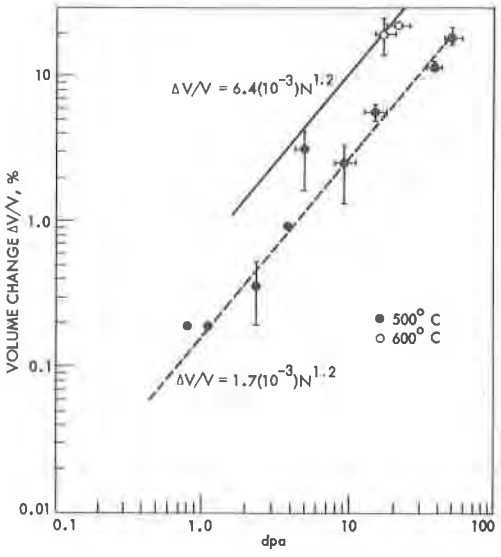

Fig. 4. Irradiation swelling varies with displacement damage for proton-irradiated 316 stainless steel containing helium.

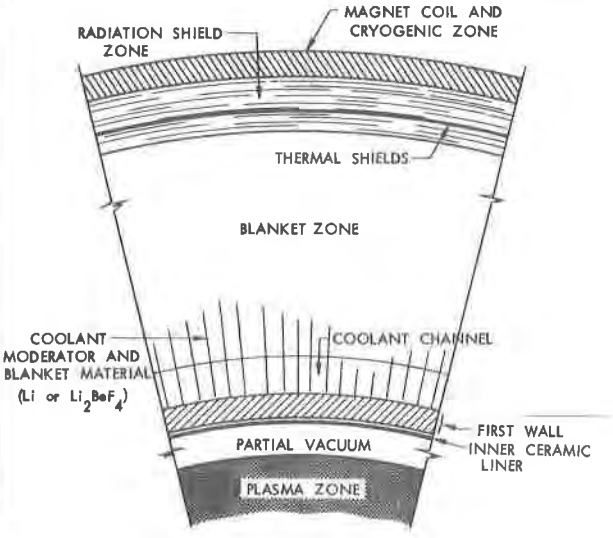

Fig. 5. Typical cross-section sector of the controlled fusion reactor using channel bank arrangements outside the first wall.

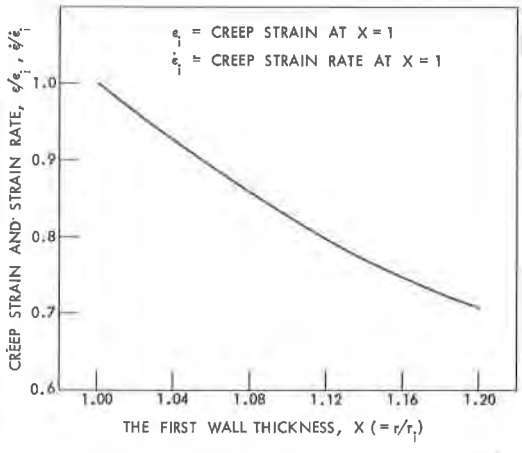

Fig. 6. Creep strain and strain rate vary with the first wall thickness.

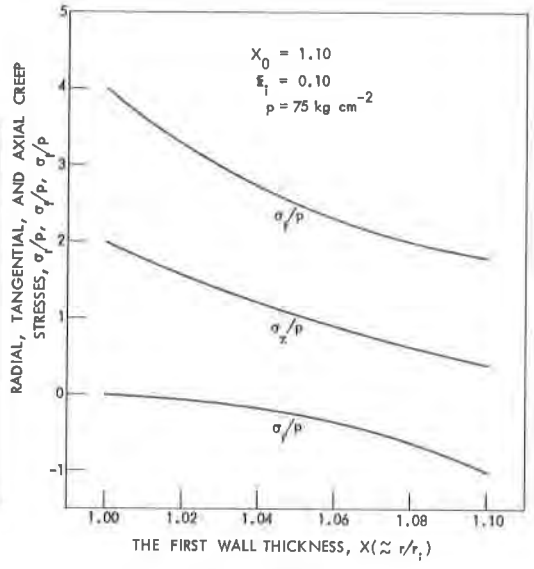

Fig. 7. Creep (radial, tangential and axial) stresses vary with the first wall thickness.

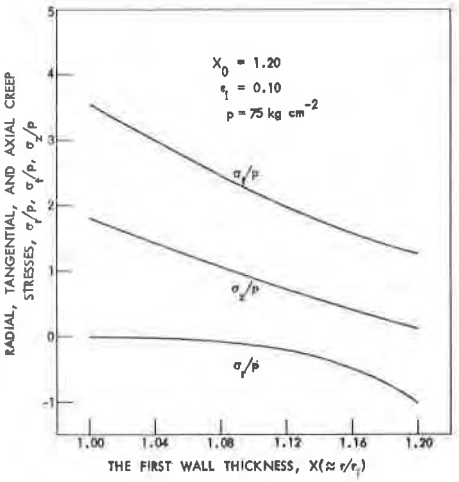

Fig. 8. Creep (radial, tangential and axial) stresses vary with the first wall thickness.

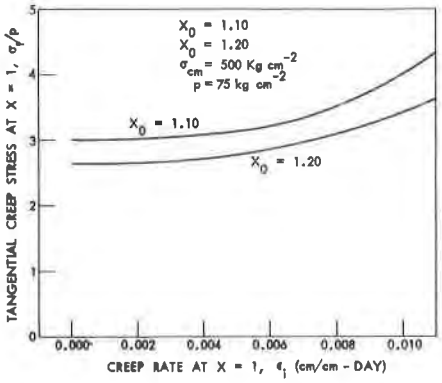

Fig. 9. Maximum tangential creep stress varies with creep rate at the inner surface of the first wall.

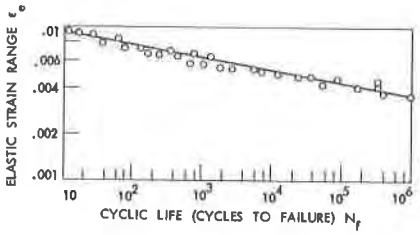

Fig. 10. Relation between elastic strain range per cycle and cyclic life (for annealed 4130 steel and others).

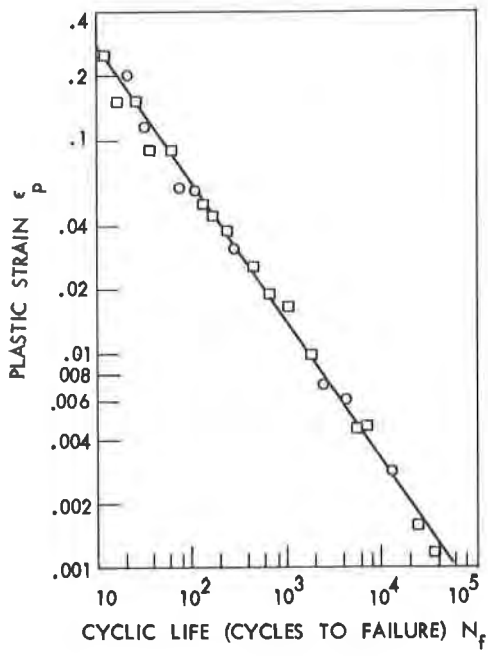

Fig. 11. Relation between plastic-strain per cycle and cyclic life (for 4130 steel and others).

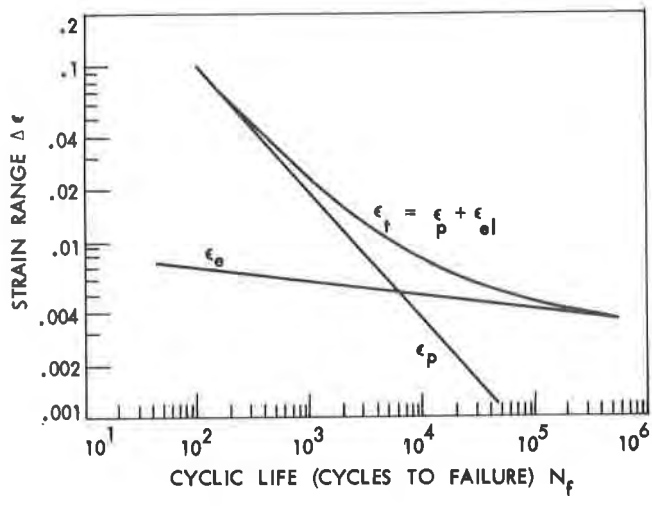

Fig. 12. Total strain range (the sum of elastic and plastic components) varies with cyclic life.